

Interplay of point and planar defects in the phase state formation and dynamics of Abrikosov vortices in $YBa_2Cu_3O_{7-\delta}$ crystals

Yu.T.Petrusenko, A.V.Bondarenko*

National Science Center "Kharkiv Institute of Physics & Technology",
1 Akademicheskaya St., 61108 Kharkiv, Ukraine
*Ukrainian State Academy of Railway Transport,
7 Feyerbach Sq., 61050 Kharkiv, Ukraine

Received July 16, 2008

The rotation of magnetic field **H** off the plane of twin boundaries (TBs) has been found to induce transition of an ordered vortex solid phase to a disordered one due to transverse deformations of vortex lines near the TBs. It has been shown that the variation of both the depinning current density J_c and the activation energy U_{pl}^{ef} corresponding to plastic vortex creep with angle $\theta \equiv \angle\mathbf{H}$,TB are not changed qualitatively with increasing concentration of point defects n_d, but this variation is strongly affected by the evolution of a kinked structure of vortex lines with the angle θ. It has been also shown that the current density J_c and energy U_{pl}^{ef} behave quite differently as the angle θ and the concentration n_d vary, and in particular, angular variation of the pinning force in the creep regime F_p, which is defined by competition between the current density J_c and the energy U_{pl}^{ef}, depends on the concentration n_d and on the driving force value.

Установлено, что поворот магнитного поля **H** с выходом из плоскости границ двойников (ГД) инициирует переход упорядоченной вихревой фазы в неупорядоченную из-за появления поперечных деформаций вихревых нитей в окрестности ГД. Показано, что изменение плотности тока депиннинга J_c и энергии активации U_{pl}^{ef}, соответствующей пластическому крипу вихрей, с углом $\theta \equiv \angle\mathbf{H}$,ГД качественно не меняется при увеличении концентрации точечных дефектов n_d, и это изменение определяется эволюцией зигзагообразной структуры вихревых нитей с углом θ. Плотность тока J_c и энергия U_{pl}^{ef} изменяются противоположным образом как с углом θ, так и с концентрацией n_d, а конкретная угловая зависимость силы пиннинга в режиме крипа F_p, которая определяется конкуренцией между плотностью тока J_c и энергией U_{pl}^{ef}, зависит от концентрации n_d и величины движущей силы.

The effect of point and planar defects on the deformation of vortex lines, on the phase state, pinning force, and dynamics of a vortex solid has been reconsidered after discovery of high-T_c materials. It has been shown that in the presence of a weak point disorder and in low magnetic fields, the elastic energy E_{el} dominates over the pinning energy E_p, and therefore, an ordered Bragg glass (BG) phase is formed, which does not contain topological defects [1]. The pinning force of the BG phase is independent of the magnetic field [2, 3] that corresponds to 1D-pinning mode. However, the energy E_{el} becomes lower than E_p with increasing point disorder or magnetic field strength, and the ordered BG phase becomes transformed into a disordered one [4]. The disordered phase contains dislocations with screw components resulting in formation of an entangled vortex solid (EVS), and thus, to realization of 3D-pinning mode. The

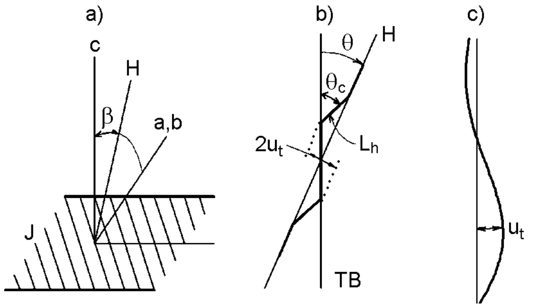

Fig. 1. (a) Sketch of measurements geometry. (b) Kinked structure of vortex line near the TB in tilted magnetic field. (c) Vortex configuration in presence of the random point disorder.

order-disorder (OD) transition is accompanied by an increase of the pinning force [5] due to dimensional crossover [6, 7] and better accommodation of the disordered phase to the pinning landscape [8].

Decoration experiments show that the superconducting order parameter (SCOP) at the twinning boundaries (TBs) in a $YBa_2Cu_3O_{7-\delta}$ compound is suppressed [9], and TBs affect the spatial distribution of vortices in both parallel and inclined to the TBs magnetic fields [10]. This is confirmed by magnetic [11, 12] and transport [13, 14] measurements, which show that the pinning force F_p changes non-monotonously with angle $\theta \equiv \angle\mathbf{H}$,TB. However, particular $F_p(\theta)$ dependences can differ one from another in different samples, thus causing discrepancy in interpretation of experimental data. This can be due to dynamics effects, which strongly affect the $F_p(\theta)$ function character in the vortex creep mode [13, 14], and by difference in the contributions to the total pinning force from point and plane defects, that is natural for different samples. The aim of this work is to study experimentally the evolution of vortex dynamics with angle θ in samples under controlled variation of point defect concentration n_d.

The measurements were performed on the $YBa_2Cu_3O_{7-\delta}$ crystal having dimensions $5\times0.2\times0.007$ mm^3 with $T_c = 93.5$ K and $\Delta T_c \cong 0.4$ K. The smallest dimension corresponded to the c-axis, the twins were oriented unidirectionally, and the average distance d between the TBs was 0.3 μm. The transport current J was applied along the ab-plane and at an angle of 45° to the TBs plane. The sample was rotated in the magnetic field so that the vector $\mathbf{H}$ was perpendicular to the vector $\mathbf{J}$, as it is shown in Fig. 1a. The resolution of angle $\beta \equiv \angle\mathbf{H},\mathbf{c}$ was better than 0.05°. The concentration of point defects was varied by low-temperature ($T \le 10$ K) irradiation with 2.5 MeV electrons [3]. The vortex dynamics was studied by measuring the current-voltage characteristics $E(J)$ for dc current at 85 K in 15 kOe magnetic field. The irradiation-measurement cycles were performed without heating the sample above 110 K, so that the effect of point defects concentration on pinning and dynamics of the vortex solid could be studied [3].

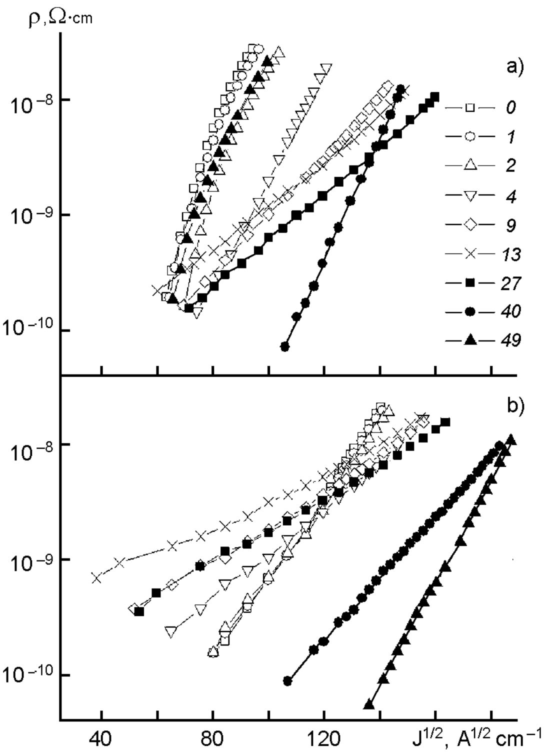

Fig. 2. Evolution of the $\rho(J)$ dependences with angle β in unirradiated crystals (a) and those irradiated with a dose $\varphi = 10^{18}$ electrons per cm^2 (b).

The measurement results plotted as $\rho(J) \equiv E(J)/J$ vs $\sqrt{J}$ are presented in Fig. 2. The Figure shows the evolution of $\rho(J)$ curves with the angle β prior to (panel a) and after (panel b) irradiation to a dose of $\varphi = 10^{18}$ electrons per cm^2. It is seen that an increase in the angle β up to 1° does not change the position of $\rho(J)$ curves, while the curves measured $\beta \ge 2°$ are separated well. First of all, it is to note that the latter fact is caused by interaction of vortices with the twins rather than by the crystal anisotropy. Indeed, the pinning force is independent of the angle β (at least up to 40°) in both non twinned crystals [12] and twinned ones [2] if the vector **H** remains parallel to the TBs plane [2]. Therefore, we believe that for small angles $\beta \le \beta_L \cong 1^\circ$, the vortex lines remain trapped by the twins, as it has been predicted by theory [15]. In our experimental geometry of measurements, the angles β and θ are related as $\sqrt{2}\sin\theta = \sin\beta$, and we obtain the value of the lock-in angle $\theta_L \cong 0.7^\circ$ agreeing with previous experimental studies [12]. We attribute the changes in pinning and dynamics of vortices observed at angles $\beta \ge 2^\circ$ to the deformation of vortex lines near the TBs, which is shown in Fig. 1b [16]. Here, at the angles θ smaller than a certain critical θ_c value, some part of the vortex line L_t is trapped by the TB, the vortex fragment L_h and the twin plane limit the angle θ_c, and far away from the TB, the vortex lines are aligned along the external field.

Previous measurements performed on the crystal in the magnetic field **H**||**c** [3] have shown that prior to irradiation, the vortex velocity $v = E/cB$ is independent of the field, and thermal creep follows the relation

$$E(J) = E_0\exp[(-U_0/k_BT)(J_c/J)], \quad (1)$$

where J_c is the depinning current density, and U_0 is the creep activation energy (in Fig. 2a, this relation manifests itself in the negative curvature of $\rho(J)$ curves). These regularities correspond respectively to 1D-pinning of the BG phase formed at a weak point disorder and contains no dislocations [1], and to elastic creep with a diverging activation energy $U(J) = U_0(J_c/J)$. As is evident from Fig. 2, both the introduction of point defects and the rotation of field off the TBs plane by the angle $\beta \ge 4^\circ$ result in a radical change in vortex dynamics: the current-voltage characteristics become straight lines being plotted as $\log[E(J)/J]$ vs $\sqrt{J}$. This means that the thermal creep is described by the relation

$$E(J) = \rho_0 J\exp\left\{(U_{pl}^{ef}/k_BT)[1 - (J/J_c)^{1/2}]\right\}, \quad (2)$$

which corresponds to plastic creep mediated by the motion of dislocations [17, 18]. The transition from elastic creep to plastic one realized in the field **H**||**c** at increasing concentration n_d is caused by the transition of the ordered BG phase into the disordered EVS one [3]. This OD transition arises due to increase in the pinning energy in the irradiated crystal, $E_p \propto n_d^{1/3}$ [15], which dominates over the elastic energy $E_{el} \cong c_L^2\varepsilon\varepsilon_0 a_0$ induced by the transverse deformations of the vortex lines $u_t = c_L a_0$ [4]. Here, c_L is the Lindemann number; ε, the anisotropy parameter; $\varepsilon_0 = (\Phi_0/4\pi\lambda)^2$, the vortex line tension; $a_0 \cong 1.07(\Phi_0/B)^{1/2}$, the intervortex distance; Φ_0, the flux quantum; and λ, the penetration depth. Transverse deformations in the irradiated sample arise due to interaction of vortex lines with the point defects, see Fig. 1c. It is believed that transverse deformations $u_t = c_L a_0$ induce transformation of the ordered vortex lattice into the disordered one. The transition from the elastic creep to plastic one observed in a non-irradiated sample at field rotation off the TBs plane through $\beta \ge 4^\circ$, can arise due to the OD transition, too. But in this case, it is initiated by transverse displacements of vortex lines u_t near the TBs, see Fig. 1b. The length of fragment $L_h \cong (\varepsilon a_0/2\sqrt{\pi})[\ln(a_0/\xi)]^{1/2}$ [16] specifies the displacement amplitude

$$u_t \cong L_h\sin(\theta_c - \theta). \quad (3)$$

For a_0(15 kOe) = 40 nm and θ = 4°, and for reasonable values of the anisotropy parameter ε = 1/5, the angle $\theta_c = 70^\circ$ [10], and the coherence length ξ(85 K) = 4 nm, we obtain the amplitude $2u_t \cong 0.2a_0$. The displacements are close to the Lindemann criterion, $u_t \approx c_L a_0$ ($c_L = 0.1 \div 0.3$), and thus can initiate the OD transition [4]. Below, it will be shown that it is just the evolution of the kinked structure that provides an explanation for angular variations of the current density J_c and the energy U_{pl}^{ef}.

In transport measurements, the J_c value can be determined by extrapolation of the normalized differential resistance $\rho_d \equiv (dE/dJ)/\rho_{BS}$ to unity [2, 3]. Substituting these values in Eq.(2) and fitting the experimental $\rho(J)$ curves to this equation, we can determine the energy U_{pl}^{ef}. The angular variation of the current density J_c and energy U_{pl}^{ef} obtained in this way are shown in Fig. 3a. The depinning current density does not change with β for $\beta < \beta_L \cong 1^\circ$, because, as it was mentioned above, the vortex lines remain trapped by the TBs. At $\beta > \beta_L$, the current J_c first rises and then drops as the angle β increases up to its maximal value J_c^{max} at β≅30°. The rise in J_c observed in the angular range $\beta_L < \beta < 30^\circ$ cannot be explained by increased pinning of the

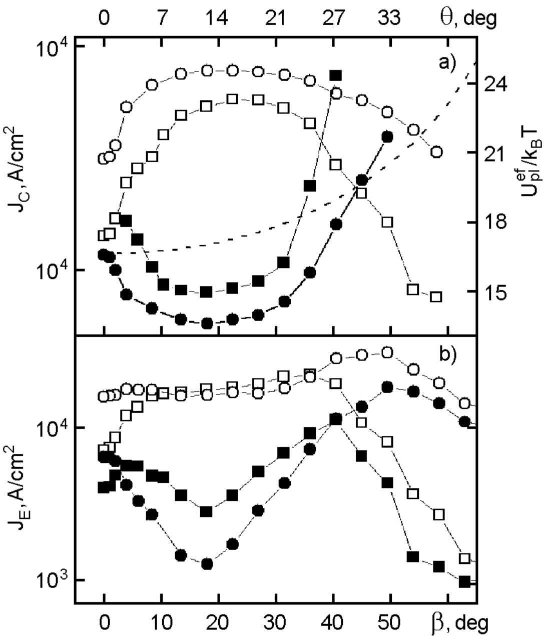

Fig. 3. (a) Angular variations of the depinning current (light symbols) and activation energy (bold symbols) in unirradiated (squares) and irradiated (circles) crystals. The dashed curve presents angular variation of the activation energy $U_{pl}(\beta) = U_{pl}{}^0\varepsilon_\beta{}^{-1/2}$ calculated for undeformed vortex lines [20]. (b) Angular variation of the threshold current J_E determined at electric field level 1 μV/cm (bold symbols) and 100 μV/cm (light symbols) in unirradiated (squares) and irradiated (circles) crystals.

trapped fragments L_t, as it was suggested in [19], because their fraction decreases as $\sin(\theta_c-\theta)$. Also, the reduced pinning in the field **H**||**c** cannot be explained by suppression of pinning by point defects, as it was assumed in [13]: the vortices located between the TBs poorly accommodate themselves to the point defects landscape due to a strong interaction with vortices trapped by the TBs. Indeed, this interpretation implies the formation of the ordered BG phase in the irradiated sample placed in the parallel field; that is in contradiction with our measurement results. Therefore, we believe that the current J_c increases due to occurrence of dislocations within spatial regions surrounding the kinks of vortex lines, where the vortex fragments L_h located at opposite sides of the TBs are shifted in the transverse direction by the distance of $2u_t{\approx}0.2a_0$. The number of kinks increases as $\sin\beta$, thus resulting in continuous increase of the dislocation concentration, and therefore, to a greater disorder of the vortex solid. Thus, in the unirradiated crystal, the increase in J_c with the angle β is caused both by the transition from a weak 1D-pinning of the BG-phase to a strong 3D-pinning of the EVS phase and by a better accommodation of disordered phases to the pinning landscape, that results in a rather large ratio $J_c(0°)/J_c{}^{max}{\cong}4.2$. In the irradiated sample, the increase in J_c is caused by the latter reason only, resulting in a smaller ratio $J_c(0°)/J_c{}^{max}{\cong}2.4$.

The reduction in current density J_c, observed at a further increase of angle β (β > 30°) is caused by a decrease in the amplitude u_t, which drops to zero at $\theta = \theta_c$ according to Eq. (3). In the absence of point defects and SCOP fluctuations within the TBs plane, a jump-like decrease in J_c at $\beta = \beta_{DO}$ might be expected. At this angle, the amplitude $2u_t$ will become smaller than c_La_0 value, thus initiating the opposite disorder-order transition. Fluctuations of both the SCOP and the concentration n_d result in the amplitude fluctuation of u_t, and therefore, in smoothing of the transition. As is seen from Fig. 3a, in the unirradiated sample, the current density J_c drops by about an order of magnitude within the angular range $\Delta\beta = 45\pm5°$, and the plastic creep gives way to the elastic one at the angle $\beta = 40°$, thus indicating the disorder-order transition. In the irradiated sample, the pinning by point defects is strong, the EVS phase is conserved up to $\beta = 50°$, and the current density J_c decreases slowly at increasing angle β due to decreasing disorder of the vortex solid.

As is seen in Fig. 3a, the angular variation of energy $U_{pl}{}^{ef}$ differs from a monotonous increase of the activation energy $U_{pl}(\beta) = U_{pl}{}^0\varepsilon_\beta{}^{-1/2}$ [20] calculated for plastic creep of undeformed vortex lines. Here, $U_{pl}{}^0 = 4\varepsilon\varepsilon_0a_0$ is the activation energy at $\beta = 0$, and $\varepsilon_\beta = (\varepsilon^2\sin^2\beta + \cos^2\beta)^{1/2}$ is the angular-dependent anisotropy parameter. The difference is justifiable, taking into account that transverse deformations reduce the activation energy by a factor of about $(1 - u_t/a_0)$ [3], and the $U_{pl}{}^{ef}$ value estimated by fitting the experimental data with Eq. (2) increases at decreasing concentration of dislocations n_D due to reduction in the number of jump attempts. Thus, we can write

$$U_{pl}^{ef}(\beta) \approx U_{pl}(\beta)(1 - u_t/a_0)f(n_D), \qquad (4)$$

where the dimensionless function $f(n_D)$ approaches unity in a strongly disordered vortex solid, and $f(n_D) \to \infty$ in the ordered vortex solid. Therefore, the angular variation of energy U_{pl}^{ef} can be interpreted as follows. At small angles β, the energy decreases due to appearance of additional transverse displacements u_t, i.e., the kinks, and also due to increased concentration of dislocations. At $\beta > 30°$, the reduction in the amplitude ut causes the disorder-order transition in the unirradiated sample, the concentration of dislocations quickly drops to zero, causing a fast increase in U_{pl}^{ef} and the transition from the plastic creep to the elastic one at angles $\beta \geq 50°$. In the irradiated sample, the point disorder is strong, the EVS phase is conserved, and the energy U_{pl}^{ef} increases gradually with the angle β due to both increasing energy $U_{pl}(\beta)$ and the decreasing amplitude u_t.

Fig. 3b shows the angular variation of threshold current density J_E determined at a fixed electric field under creep conditions. It is seen that in the deep creep mode (E = 1 μV/cm), it correlates with the angular variation of the activation energy U_{pl}^{ef} up to the angles β of 40 to 50°, and with an increased driving force (E = 100 μV/cm) it correlates neither with $J_c(\beta)$ nor with $J_c(\beta)$ function. This behavior is expected because the current density J_E is defined by competition between the current density J_c and energy U_{pl}^{ef}, which oppositely very with the angle β.

Note that previous estimations of the angle θ_c and the interpretation of the TBs effect on the vortex solid pinning in the $YBa_2Cu_3O_{7-\delta}$ superconductor were based primarily on the angular variation of the pinning force under creep conditions [12–15], and in the transport studies, the angular variations of depinning current and activation energy were discussed only in Ref. [20]. However, in that work, it was impossible to separate the contributions from point defects and planar defects, because the vortex dynamics in the fields **H**||**c** was defined by the release of vortices from the TBs potential wall, and the experimental data were discussed in the context of the collective pinning theory. It should be also mentioned that our measurements do not provide the exact value of angle θ_c, but we may suggest that the TBs affect pinning at least up to $\beta = 50°$. That is in agreement with some previous studies of vortex dynamics [20, 21], and agrees with the value of $\beta = 75°$ derived from direct observations of vortex lattice in inclined fields [10].

To conclude, it has been found that in samples with a weak point disorder, the kinked vortex lines structure, which is formed in magnetic fields inclined to the TBs, causes the transition from the ordered Bragg-glass phase in parallel fields to the entangled vortex solid in tilted fields. It is also shown that it is just evolution of the kinked vortex structure that specifies the angular variation of the depinning current density and the activation energy corresponding to plastic creep. Increase of the point defects concentration causes formation of the disordered vortex solid in parallel to the TBs field, and increases interval of the angles β where the disordered vortex solid is conserved. It is shown that increase of the defects concentration raises the depinning current density and decreases activation energy corresponding to the plastic creep of the vortex lattice.

References

1. T.Giamarchi, P.Le Doussal, *Phys. Rev. Lett.*, **72**, 1530 (1994).
2. A.V.Bondarenko, A.A.Prodan, M.A.Obolenskii et al., *Low Temp. Phys.*, **27**, 339 (2001) .
3. A.V.Bondarenko, A.A.Prodan, Yu.T.Petrusenko et al., *Phys. Rev.*, **B64**, 092513 (2001).
4. D.Ertas, D.R.Nelson, *Physica*, **C272**, 79 (1996).
5. B.Khaikovich, E.Zeldov, D.Majer et al., *Phys. Rev. Lett.*, **76**, 2555 (1996).
6. R.Wodenweber, P.Kes, *Phys. Rev.*, **B34**, 494 (1986).
7. E.H.Brandt, *Phys. Rev.*, **B34**, 6514 (1986).
8. M.Gingras, D.Huse, *Phys. Rev.*, **B53**, 15193 (1996).
9. L.Ya.Vinnikov, L.A.Gurevich, G.A.Yemel'chenko, Yu.A.Ossipyan, *Solid St. Commun.*, **67**, 421 (1988).
10. J.A.Herbsommer, G.Nieva, J.Luzuriaga, *Phys. Rev.*, **B62**, 3534 (2000).
11. L.J.Swartzendruber, A.R.Roitburg, D.L.Kaiser et al., *Phys. Rev. Lett.*, **64**, 483 (1990).
12. A.A.Zhukov, G.K.Perkins, J.V.Thomas et al., *Phys. Rev.*, **B56**, 3481 (1997).
13. V.F.Solovjov, V.M.Pan, H.C.Freyhardt, *Phys. Rev.*, **B50**, 13724 (1994).
14. V.M.Pan, V.F.Solovjov, H.C.Freyhardt, *Physica*, **C279**, 18 (1997).
15. W.K.Kwok, J.A.Fendrich, V.M.Vinokur et al., *Phys. Rev. Lett.*, **76**, 4809 (1996).
16. G.Blatter, M.V.Feigel'man, V.B.Geshkenbein et al., *Rev. Mod. Phys.*, **66**, 1125 (1994).
17. J.P.Hirth, J.Lothe, Theory of Dislocations, John Wiley & Sons, New York (1982), Chap.15.

18. A.Abulafia, A.Shaulov, Y.Wolfus et al., *Phys. Rev. Lett.*, **77**, 1596 (1996).
19. A.V.Bondarenko, V.A.Shklovskij, R.V.Vovk et al., *Fiz. Nizk. Temp.*, **23**, 1281 (1997).
20. A.V.Bondarenko, M.G.Revyakina, A.A.Prodan et al., *Fiz. Nizk. Temp.*, **27**, 275 (2001).
21. R.Hiergeist, R.Hergt, *Phys. Rev.*, **B55**, 3258 (1997).

Взаємний вплив точкових та плоских дефектів на формування фазового стану та на динаміку абрикосовських вихорів у кристалах $YBa_2Cu_3O_{7-\delta}$

Ю.Т.Петрусенко, А.В.Бондаренко

Встановлено, що поворот магнітного поля **H** з виходом з площини меж двійників (МД) ініціює перехід упорядкованої вихрової фази у неупорядковану внаслідок появи поперечних деформацій вихрових ниток в околі МД. Показано, що зміна густини струму депінінгу J_c та енергії активації U_{pl}^{ef}, яка відповідає пластичному крипу вихорів, з кутом $\theta \equiv \angle\mathbf{H}$,МД якісно не змінюється при збільшенні концентрації точкових дефектів n_d, і ця зміна визначається еволюцією зигзагоподібної структури вихрових ниток з кутом θ. Густина струму J_c та енергія U_{pl}^{ef} змінюються у протилежних напрямках як з кутом θ, так і з концентрацією n_d, а конкретна кутова залежність сили пінінгу у режимі крипу F_p, яка визначається конкуренцією між густиною струму J_c та енергією U_{pl}^{ef}, залежить від концентрації n_d та від величини рушійної сили.